metals

MDPI

Review

Friction Stir Welding of Dissimilar Aluminum Alloy Combinations: State-of-the-Art

Vivek Patel [1,2], Wenya Li [1,*], Guoqing Wang [3], Feifan Wang [3], Achilles Vairis [1,4] and Pengliang Niu [1]

1 State Key Laboratory of Solidification Processing, Shaanxi Key Laboratory of Friction Welding Technologies, School of Materials Science and Engineering, Northwestern Polytechnical University, Xi'an 710072, China; profvvp@yahoo.com or vivek.patel@sot.pdpu.ac.in (V.P.); vairis@staff.teicrete.gr (A.V.); penglniu@126.com (P.N.)

2 Department of Mechanical Engineering, School of Technology, Pandit Deendayal Petroleum University, Gandhinagar 382007, India

3 China Academy of Launch Vehicle Technology, Beijing Institute of Astronautical Systems Engineering, Beijing 100076, China; vivsforyou@gmail.com (G.W.); wangifw@hotmail.com (F.W.)

4 Mechanical Engineering Department, TEI of Crete, Heraklion 71004, Greece

* Correspondence: liwy@nwpu.edu.cn; Tel.: +86-29-8849-5226; Fax: +86-29-8849-2642

Received: 17 January 2019; Accepted: 11 February 2019; Published: 26 February 2019

Abstract: Friction stir welding (FSW) has enjoyed great success in joining aluminum alloys. As lightweight structures are designed in higher numbers, it is only natural that FSW is being explored to join dissimilar aluminum alloys. The use of different aluminum alloy combinations in applications offers the combined benefit of cost and performance in the same component. This review focuses on the application of FSW in dissimilar aluminum alloy combinations in order to disseminate research this topic. The review details published works on FSWed dissimilar aluminum alloys. The detailed summary of literature lists welding parameters for the different aluminum alloy combinations. Furthermore, auxiliary welding parameters such as positioning of the alloy, tool rotation speed, welding speed and tool geometry are discussed. Microstructural features together with joint mechanical properties, like hardness and tensile strength measurements, are presented. At the end, new directions for the joining of dissimilar aluminum alloy combinations should guide further research to extend as well as to improve the process, which is expected to raise further interest on the topic.

Keywords: aluminum; dissimilar; friction stir welding; FSW; hardness; microstructure; tensile

1. Introduction

Friction stir welding (FSW) is a solid state welding process which was invented at The Welding Institute (TWI) in UK in 1991 [1]. FSW is regarded as an environmentally friendly and energy efficient joining technique providing one of the best alternatives to fusion welding in order to produce a good combination of microstructure and properties in the joints. FSW has already proved its superiority in joining aluminum (Al) alloys as well as magnesium (Mg) alloys over fusion welding processes because of its solid-state nature. FSW uses a non-consumable rotating tool which has a shoulder and a pin (or more formally probe) at its end which plunges into the base material (BM) and advances in the welding direction [2], as shown in Figure 1. During the process, the shoulder touches the top surface of the BM and the pin moves yielded material around it. As a result of this action, heat is generated by frictional and plastic deformation of the BM by advancing the rotating tool. The shoulder of the tool has a forging action as it restricts the expulsion of plasticized material from the BM, while the pin extrudes material and produces a material flow between the advancing side (AS) and the retreating

side (RS) of the joint. FSW has shown great potential in welding Al alloys for structural applications. More recently, Ma et al. [3] published a critical review paper on recent developments in FSW of Al alloys. Al alloys have remained the prime selection for structural material in aerospace, shipbuilding and automotive industries for their excellent strength to weight ratio. In order to improve performance while controlling the cost of Al alloys in these industries, there is an increasing demand to weld dissimilar Al joints with FSW. Because of the different physical and chemical properties in dissimilar Al alloy combinations, challenges such as solidification cracking, porosity, formation of intermetallic and so forth, are present. Therefore, the FSW of dissimilar Al alloy combinations has gained attention over the recent years, demonstrating the potential of the process to join these. The present review aims to discuss and analyze the available literature on FSWed dissimilar Al alloy combinations so far.

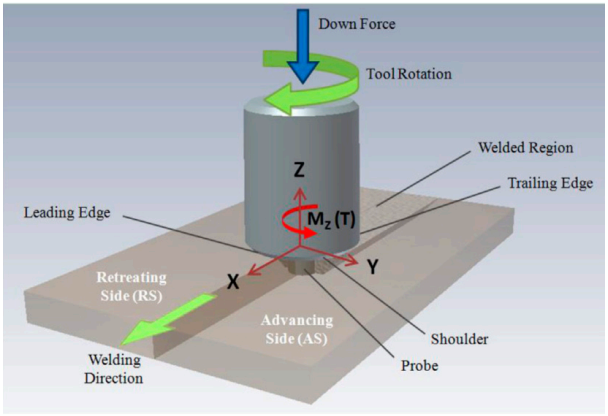

Figure 1. Schematic of friction stir welding, reproduced from [4], with permission from Elsevier, 2014.

2. General Progress in FSW of Dissimilar Al-Al Combinations

There are review papers available on FSW of same Al alloy joints, which discuss various aspects of the process such as tool design, process parameters, heat generation, microstructure and mechanical properties [4–11]. The number of research papers on FSW of dissimilar Al alloy joints published to date is shown in Figure 2 (search on 15 December 2017 found 68 papers from Web of Science). The vast majority of the publications has been in the past 5 years, reaching a peak on 2018. In addition, Magalhães et al. [12] studied research and the extent of industrial application of FSW of similar and dissimilar material joints as shown in Figure 3. The similar material joints of Al alloys are being studied to a far larger extent compared to other alloys and the same trend is observed in the dissimilar material combinations. This trend observed literature clearly identifies the interest on the FSW of dissimilar Al alloy joints, which is expected to increase over the coming years.

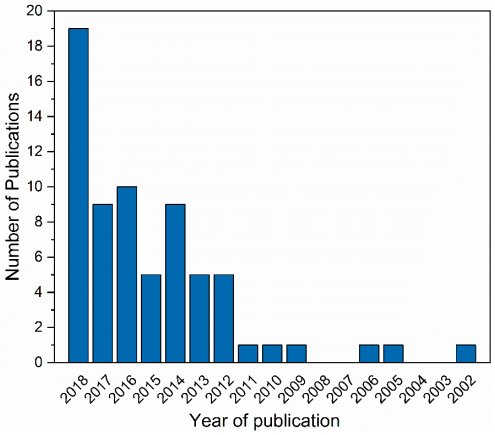

Figure 2. Journal papers published on FSW of dissimilar Al alloy joints.

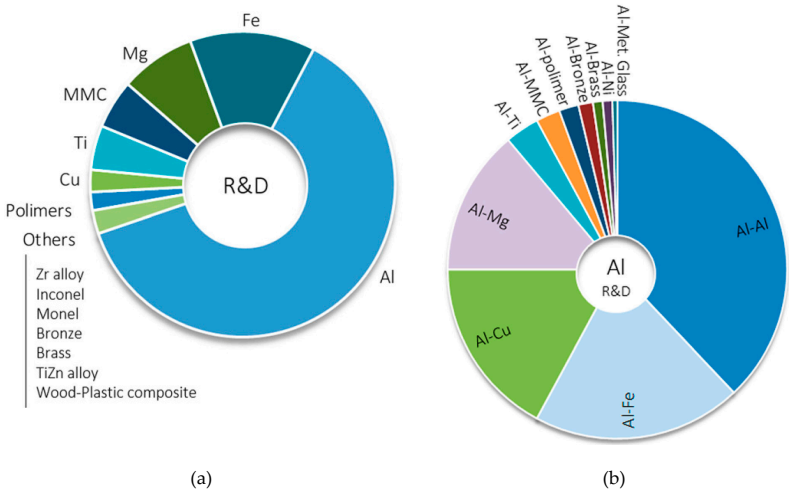

(a) (b)

Figure 3. Papers on FSW: (**a**) same material joints and (**b**) dissimilar materials joints, reproduced from [12], with permission from Taylor & Francis, 2017.

All papers from the top 10 ranked journals published on FSW, classified as Q1 by Scimago Journal & Country Rank.

Summary of Published Works

In order to identify the key findings on various aspects a summary of existing literature follows (Table 1). For the FSW of dissimilar Al alloy combinations there are the preliminary welding parameters such as the BM placement, the tool rotational speed and welding speed. The placement of the BM affects material flow, while rotational and welding speeds control heat input on both sides of the joint during welding. All of these parameters have been investigated for the different material combinations (see Table 1). In addition, the effects of welding parameters on the mechanical properties that is, the hardness and the joint strength have been investigated. As it can be seen a number of studies have been performed on the effect of the placement of BM (i.e., whether a particular material is placed on the AS or the RS side) on the material flow and the resulting microstructure in the SZ and the mechanical properties of the weld. Other papers have focused on the effect of tool geometry that is, shoulder diameter to pin diameter ratio and pin profile (cylindrical, conical, polygonal) on the microstructure and mechanical properties of the weld.

Table 1. Summary of FSW of dissimilar Al alloy joints studied in literature.

No.	Author (s)	Alloy Combinations	Thick (mm)	Welding Parameters				Objective of Study
				Alloy Positioning		Rotation Speed (rpm)	Welding Speed (mm/min)	
				AS	RS			
1	Niu, et al. [13]	2024-T351 & 5083-H112	6.35	2024	5083	600	150	Strain hardening behavior and mechanism
2	Niu, et al. [13]	7075-T651 & 2024-T351	6.35	7075	2024	600	150	Strain hardening behavior and mechanism
3	Hasan, et al. [14]	7075-T651 & 2024-T351	6	Both	both	900	150	Effect of pin flute radius and alloy positioning
4	Ge, et al. [15]	7075-T6 & 2024-T3 Lap joint: 7075-upper; 2024-lower	3	NA	NA	600	30, 60, 90, 120	Effect of pin length and welding speed
5	Kalemba–Rec, et al. [16]	7075-T651 & 5083-H111	6	Both	Both	280, 355, 450, 560	140	Influence of tool rotation speed, pin geometry and alloy positioning
6	Safarbali, et al. [17]	2024-T4 & 7075-T6	4	2024	7075	1140	32	Effect of post-weld treatment
7	Palanivel, et al. [18]	6351-T6 & 5083-H111	6	6351	5083	800, 1000, 1200	45, 60, 75	Optimization of shoulder profile, rotational speed and welding speed
8	Hamilton, et al. [19]	2017A-T451 & 7075-T651	6	Both	Both	355	112	Phase transformation maps
9	Gupta, et al. [20]	5083-O & AA6063-T6	6	NR	NR	700, 900, 1100	40, 60, 80	Optimization of tool geometry, rotational speed and welding speed
10	Huang, et al. [21]	5052&AlMg$_2$Si	8	Al-Mg$_2$Si	5052	1000	80	Microstructure and mechanical properties
11	Moradi, et al. [22]	2024-T351& 6061-T6	6	2024	6061	800	31.5	Texture evolution
12	Prasanth and Raj [23]	6061-T6 & 6351-T6	6.35	NR	NR	600, 900, 1200	30, 60, 90	Optimization of rotational speed, welding speed and axial force
13	Azeez and Akinlabi [24]	6082-T6 & 7075-T6	10	7075	6082	950, 1000	80, 100	Double-sided weld
14	Azeez, et al. [25]	6082-T6 & 7075-T6	10	7075	6082	950, 1000	80, 100	Single-sided weld
15	Peng, et al. [26]	6061-T651 & 5A06-H112	5	6061	5A06	600, 900, 1200	100, 150	Nanoindentation hardness and fracture behavior
16	Das and Toppo [27]	6101-T6 & 6351-T6	12	6101	6351	900, 1100, 1300	16	Influence of rotational speed on temperature and impact strength
17	Sarsilmaz [28]	2024-T3 & 6063-T6	8	2024	6063	900, 1120, 1400	125, 160, 200	Microstructure, tensile and fatigue behavior
18	Kookil, et al. [29]	2219-T87 & 2195-T8	7.2	Both	Both	400, 600, 800	120, 180, 240, 300	Effect of rotational speed and welding speed
19	Hamilton, et al. [30]	2017A-T451 & 7075-T651	6	Both	Both	355	112	Positron lifetime annihilation spectroscopy
20	Kopyscianski, et al. [31]	2017A-T451 & Cast AlSi9Mg	6	2017A	AlSi9Mg	355	112	Microstructural study
21	Ghaffarpour, et al. [32]	5083-H12 & 6061-T6	1.5	6061	5083	700, 1800, 2500	25, 30, 212.5, 400	Optimization of rotational speed, welding speed and tool dimensions

Table 1. *Cont.*

No.	Author (s)	Alloy Combinations	Thick (mm)	Welding Parameters				Objective of Study
				Alloy Positioning		Rotation Speed (rpm)	Welding Speed (mm/min)	
				AS	RS			
22	Bijanrostami, et al. [33]	6061-T6 & 7075-T6	5	6061	7075	1000, 1375, 1750, 2125, 2500	50, 125, 200, 275, 350	Underwater FSW: optimizations of rotational and welding speeds on tensile properties
23	Kasman, et al. [34]	5083-H111& 6082-T6	5	NR	NR	400, 500, 630, 800	40, 50, 63, 80	Effect of probe shape, rotational speed, welding speed.
24	Palanivel, et al. [35]	5083-H111 & 6351-T6	6	6351	5083	800-1200	45-85	Macrostructure examination at different rotational and welding speeds
25	Doley and Kore [36]	5052 & 6061	1, 1.5	6061	5052	1500	63, 98	Study of welding speed
26	Saravanan, et al. [37]	2024-T6 & 7075-T6	5	2024	7075	1200	12	Effect of shoulder diameter to probe diameter
27	Yan, et al. [38]	Al-Mg-Si & Al-Zn-Mg	15	Both	Both	800	180	Effect of alloy positioning on fatigue property
28	Yan, et al. [39]	Al-Mg-Si & Al-Zn-Mg	15	Both	Both	800	180	Study of Fatigue behavior
29	Hamilton, et al. [40]	2017A-T451 & 7075-T651	6	Both	Both	355	112	Numerical simulation
30	Zapata, et al. [41]	2024-T3 & 6061-T6	4.8	2024	6061	500, 650, 840	45, 65	Effect of rotational and welding speeds on residual stress
31	Sun, et al. [42]	UFG 1050 & 6061-T6	2	Both	Both	800	400, 600, 800, 1000	Microstructure and mechanical properties at different welding speeds
32	Texier, et al. [43]	2024-T3 & 2198-T3	3.18	2198	2024	NR	NR	Heterogeneities in microstructure and tensile properties at the shoulder-affected regions
33	Rodriguez, et al. [44]	6061-T6 & 7050-T7451	5	7050	6061	270, 340, 310	114	Fatigue behavior
34	Yoon, et al. [45]	6111-T4 & 5023-T4 Lap joint	1	NA	NA	1500 1000	100 700	Mechanism of onion ring formation
35	Rodriguez, et al. [46]	6061-T6 & 7050-T7451	5	7050	6061	270, 340, 310	114	Microstructure and mechanical properties
36	Ilangovan, et al. [47]	5086-O & 6061-T6	6	6061	5086	1100	22	Effect of probe profiles
37	Reza–E–Rabby, et al. [48]	2050-T4 & 6061-T651	20	Both	Both	150 300 300	101 203 406	Effect of probe features
38	Donatus, et al. [49]	5083-O & 6082-T6	NR	5083	6082	400	400	Anodizing behavior
39	Karam, et al. [50]	A319 & A413 cast	10	A413	A319	630, 800, 1000	20, 40, 63	Influence of rotational and welding speed
40	Ipekoglu and Cam [51]	7075-O & 6061-O 7075-T6 & 6061-T6	3.17	6061	7075	1000 1500	150 400	Effect of initial temper conditions and postweld heat treatment
41	Cole, et al. [52]	6061-T6 & 7075-T6	4.6	Both	Both	700-1450	100	Effect of temperature
42	Song, et al. [53]	2024-T3 & AA7075-T6 Lap joint	5	NA	NA	1500	50, 150, 225, 300	Effect of alloy positioning and welding speed on defects and mechanical properties

Table 1. *Cont.*

No.	Author (s)	Alloy Combinations	Thick (mm)	Welding Parameters				Objective of Study
				Alloy Positioning		Rotation Speed (rpm)	Welding Speed (mm/min)	
				AS	RS			
43	Jannet and Mathews [54]	5083-O & 6061-T6	6	6061	5083	600, 750, 900	60	Effect of rotational speed
44	Palanivel, et al. [55]	6351-T6 & 5083-H111	6	6351	5083	950	36, 63, 90	Effect of welding speed
45	Jonckheere, et al. [56]	2014-T6 & 6061-T6	4.7	Both	Both	500, 1500	90	Effect of alloy positioning and tool offset on temperature and hardness
46	Palanivel, et al. [57]	6351-T6 & 5083-H111	6	6351	5083	600-1300	36-90	Optimization of process parameters (probe shapes, rotational and welding speeds, axial force) for UTS
47	Ghosh, et al. [58]	A356 & 6061-T6	3	6061	A356	1000	70-240	Effect of welding speed
48	Velotti, et al. [59]	2198-T351 & 7075-T6 Lap joint	3 & 1.9	NA	NA	830	40	Stress corrosion cracking investigation
49	Koilraj, et al. [60]	2219-T87 & 5083-H321	6	2219	5083	400-800	15-60	Optimization of process parameters (probe shapes, rotational and welding speeds, shoulder to probe diameter ratio) for UTS
50	Dinaharan, et al. [61]	6061 cast &6061 rolled	6	Both	Both	800, 1000, 1200, 1400	50	Effect of rotational speed and alloy positioning
51	Palanivel, et al. [62]	6351-T6 & 5083-H111	6	6351	5083	600, 950, 1300	60	Effect of rotational speed and probe profile
52	Song, et al. [63]	5052-H34 & 5023-T4	~1.5	5052	5023	1500	100-700	Liquation cracking study
53	Ghosh, et al. [64]	A356 & 6061-T6	3	6061	A356	1000, 1400	80, 240	Effect of rotational and welding speed
54	Kim, et al. [65]	5052-H34 & 5023-T4	1.5 & 1.6	Both	Both	1000, 1500	100, 200, 300, 400	Effect of alloy positioning
55	Prime, et al. [66]	7050-T7451 & 2024-T351	25.4	2024	7050	NR	50.8	Residual stress study
56	Miles, et al. [67]	5182-O & 5754-O 5182-O & 6022-T4 5754-O & 6022-T4	~2	NR	NR	500, 1000, 1500	130, 240, 400	Formability study
57	Ouyang and Kovacevic [68]	6061-T6 & 2024-T3	12.7	NR	NR	637	133	Material flow study

3. Welding Parameters

3.1. Positioning of Alloy

The placement of the alloy affects material flow as it strongly influences material stirring and mixing. This can be crucial in the final joint microstructure when the BM combination selected have significant differences in mechanical properties [69,70]. As the material flow during FSW is quite complex on its own, the placement of materials becomes an important parameter in welding, similar to the importance of the rotation and the welding speeds (see Table 1). For example Yan et al. [38] showed this for the Al-Zn-Mg and the Al-Mg-Si combination. There is an interesting material flow resistance behavior at the RS due to the difference in mechanical properties. When the Al-Zn-Mg alloy is placed at the AS, there was limited movement of the Al-Mg-Si alloy material to the AS side because of its stronger ability to flow as shown in Figure 4a. When the Al-Mg-Si was placed at the RS, there was no RS material (Al-Zn-Mg) flow to AS due to the strong resistance to flow by this high strength material as shown in Figure 4b. As it can be seen from Figure 4, the zig-zag line bonding interface formed due to excellent material mixing. The bonding interface may have vortex type in case of poor combination of rotational speed and welding speed and it becomes more prominent for BMs with significant difference in the properties. Niu et al. [71] investigated an AA2024-AA7075 joint and found that the top section of the SZ was composed of the BM of RS, whereas the middle and bottom sections by the BM of AS as shown in Figure 5. Kim et al. [65] also showed that by placing the high strength Al alloy on the AS generates excessive agglomerations and defects due to limited material flow. In essence, the high strength Al should be placed at the RS to minimize the effect of the resistance to material flow.

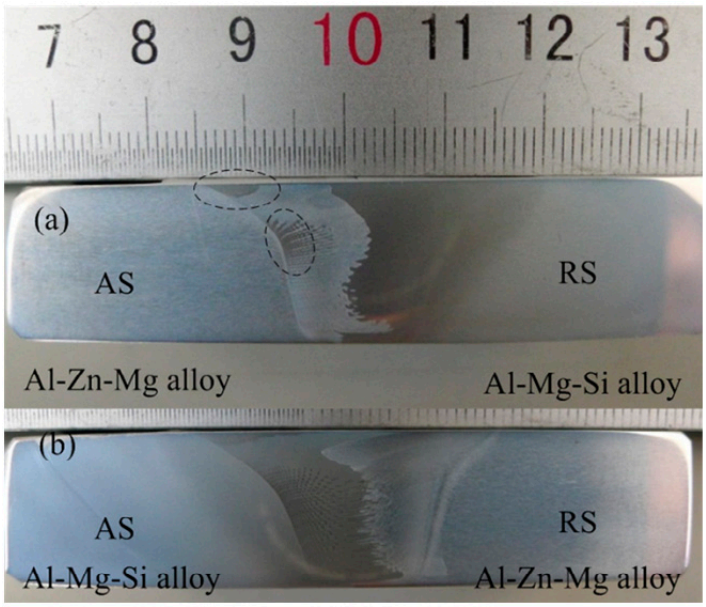

Figure 4. Cross sectional photos of the joints: (**a**) AS: Al-Zn-Mg and (**b**) AS: Al-Mg-Si, reproduced from [38], with permission from Elsevier, 2016.

In the case of the lap joint, the BM placement affects the material flow and leads to the generation of the ubiquitous hook defect. Now the material movement is in an upward direction that is, from the bottom sheet to the top sheet, creating hook defects of various sizes. As expected, in addition to the rotation and welding speed, the placement of the BM affects the hook size as well [53,72–74]. As it can be seen from Figure 6, the hook height is larger at the RS when the AA2024 is placed at the top, while it decreases when the AA7075 is placed as a top plate.

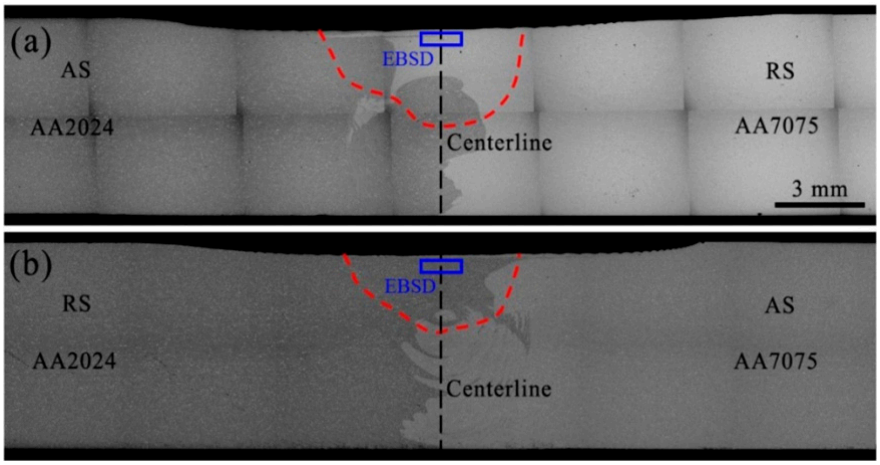

Figure 5. Cross-sectional SEM macrostructure of the AA2024-AA77075 joints: (**a**) AS: AA2024 and (**b**) AS: AA7075, reproduced from [71], with permission from Elsevier, 2019.

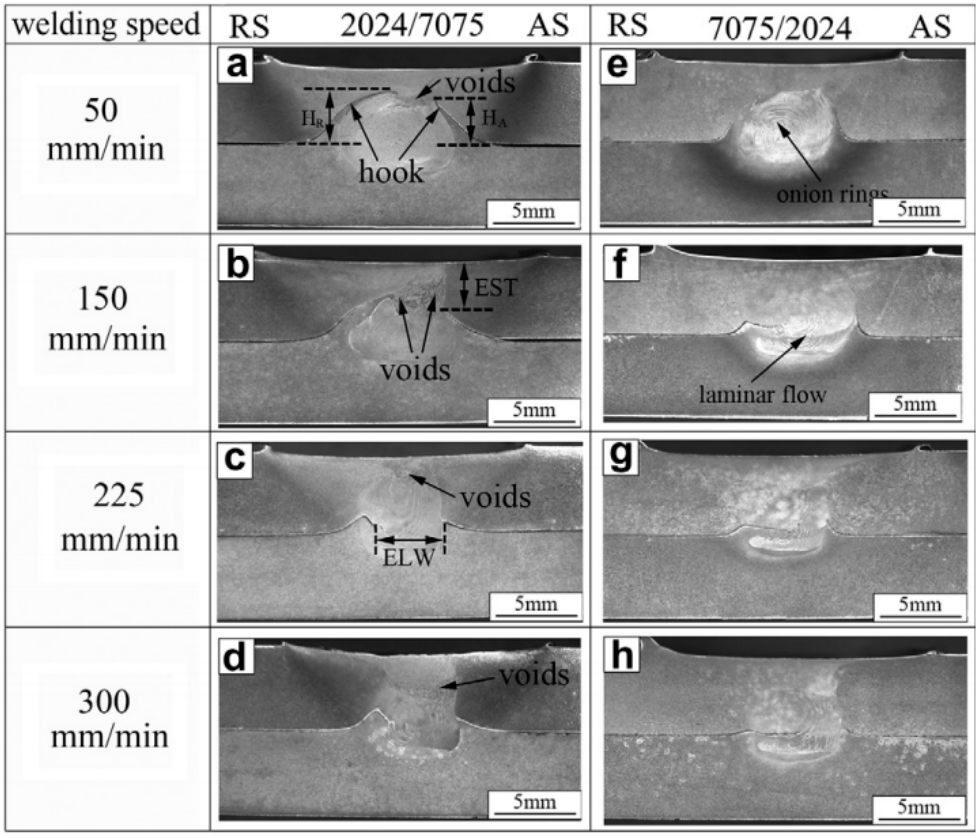

Figure 6. Cross sections of lap joints produced at various welding speeds: AA2024 as top plate (**a**) 50, (**b**) 150, (**c**) 225, (**d**) 300 mm/min; AA7075 as top plate (**e**) 50, (**f**) 150, (**g**) 225, (**h**) 300 mm/min, reproduced from [53], with permission from Elsevier, 2014.

3.2. Tool Rotation and Welding Speeds

Tool rotation and welding speeds control heat generation or heat input as they relate to the material plastic flow during FSW. The tool rotation speed affects the intensity of plastic deformation and through this affects material mixing. Kalemba-Rec et al. [16] showed a proportional relationship between material mixing and tool rotation speed for a dissimilar AA7075-AA5083 joint. However, very large rotation speeds lead to numerous imperfections such as poor surface (flash), voids, porosity,

tunneling or formation of wormholes because of the excessive heat input [75–77], as shown in Figure 7. Low welding speeds increase heat input and are associated with defects like tunneling [55,58,75,78,79]. It is therefore necessary to select the appropriate combination of tool rotation and welding speed for a defect free joint with a good metallurgical bond and mechanical properties. As it can be seen in Table 1, quite a lot of papers have focused on the optimization of these parameters for different combinations of Al alloys [23,29,32,33,35,36,41,42,50,54,55,58,64,80].

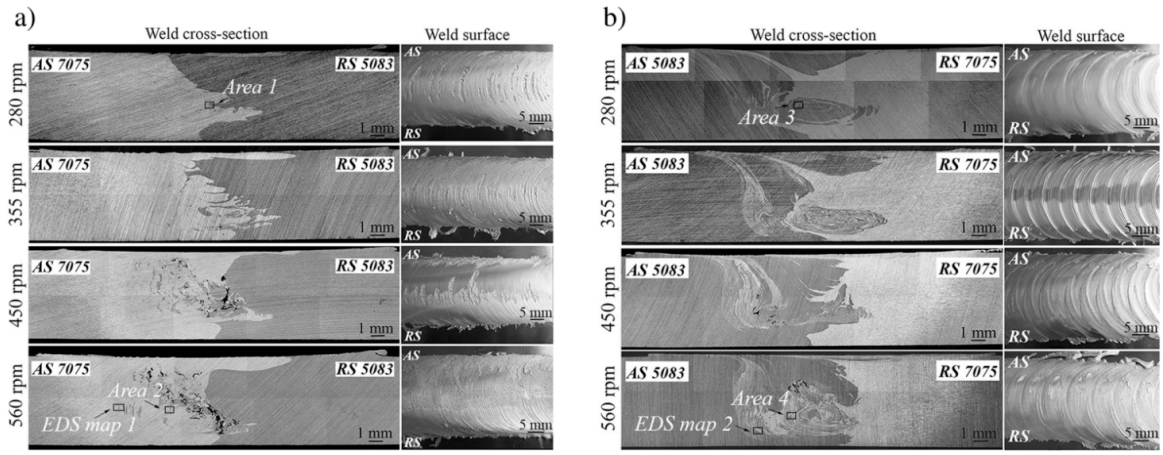

Figure 7. Cross sectional and top surface photos of an (**a**) AS 7075–RS 5083 weld and (**b**) an AS 5083–RS 7075 weld (AS—advancing side, RS—retreating side), whereas marked areas indicate further microstructural analysis; Triflute pin employed [16], with permission from the authors.

3.3. Tool Geometry

The geometry of the shoulder and the pin profile govern heat generation and material flow during welding [81]. The shoulder contributes to a large extent to heat input due to its size. The common shoulder profiles employed are the flat, the concave and the convex. Additional features on the pin such as a spiral or a groove improve frictional behavior as well as material flow. Palanivel et al. [18] reported on the effect of shoulder profiles on the AA5083-AA6351 combination by using three different shoulder features, the partial impeller (PI), the full impeller (FI) and the flat grove (FS) as shown in Figure 8. The full impeller shoulder tool produced the optimum mechanical strength due to the enhanced material flow it produced. The pin profile greatly affects material stirring and mixing. Cylindrical or conical pin profiles which may have features like threads or threads with flats have been used for dissimilar Al alloy combinations as shown in Figure 8. When used without threads a smaller surface is provided to the material, while the threaded and flat features on it increase the contact area while threads guide material flow around the pin in a rotational as well as a translation direction [14,16,47,82]. The polygonal pin profiles produce pulses in the flow during material stirring and mixing, leading to material adhering to the pin [83–86]. This pulsating effect hinders material flow significantly in the case of dissimilar Al alloy combinations. It is therefore recommended to use a cylindrical or a conical pin profile with various features in the dissimilar Al alloy joints for good material flow to produce sound joints.

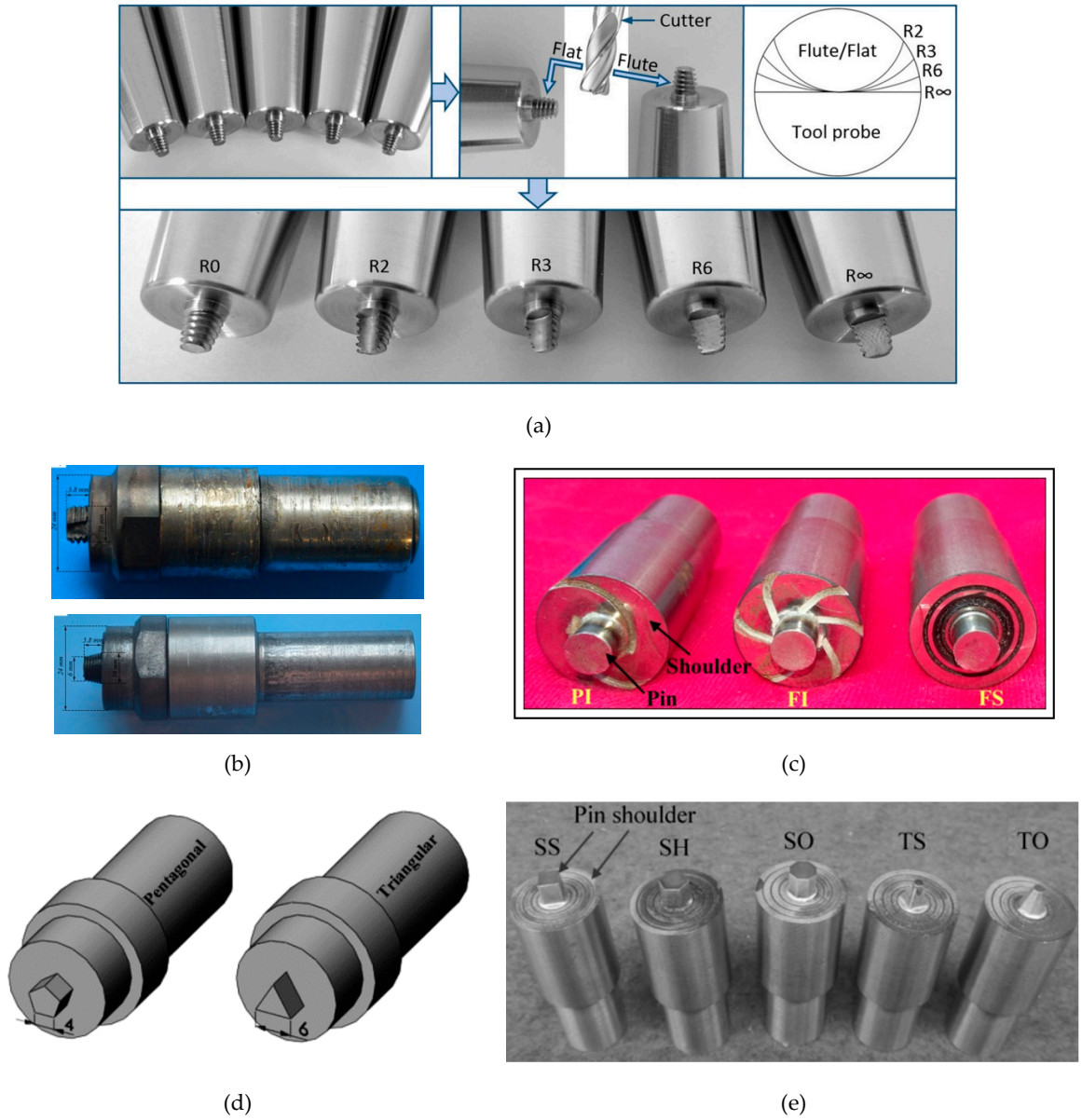

Figure 8. Tools of different geometries used in different Al alloy combinations. (**a**) AA2024-AA7075, reproduced from [14], with permission from Springer, 2018; (**b**) AA5083-AA7075, reproduced from [16], with permission from Springer, 2018; (**c**) AA5083-AA6351, reproduced from [18], with permission from SAGE, 2018; (**d**) AA5083-AA6082 [34], with permission from the authors; (**e**) AA5083-AA6351 [57], with permission from Springer, 2013.

4. Microstructure Evolution

The typical microstructure of a FSW joint consists of three distinct zones that is, HAZ, TMAZ and SZ [87,88]. These zones form depending on the thermal and mechanical deformation that the tool induces during welding. The SZ undergoes extensive grain refinement, producing fine grain microstructures, while the TMAZ has an elongated grain structure [89,90]. The microstructure evolution depends on the welding parameters (as discussed in the previous section), as the material movement or flow plays a more important role in the case of dissimilar material combinations compared to same material joints. The appropriate selection of all process parameters results in excellent material mixing on the both sides (AS and RS) of the joint and produces a sound weld. Recently, a comprehensive EBSD investigation for the AA5083-AA2024 joint was reported by

Niu et al. [91], as shown in Figure 9. As it can be seen from the EBSD orientation maps (Figure 9a–d), tilted and elongated grains in the TMAZ and fine grains d in the SZ developed due to dynamic recrystallization. Grain boundary orientations also varied in all three zones as shown in Figure 9(e–h). A higher fraction of large (>10°) angular grain boundaries was present in the SZ, while more of low (2–10°) angular grain boundaries were present in HAZ. Also, a more intense texture in the SZ was formed compared to other zones.

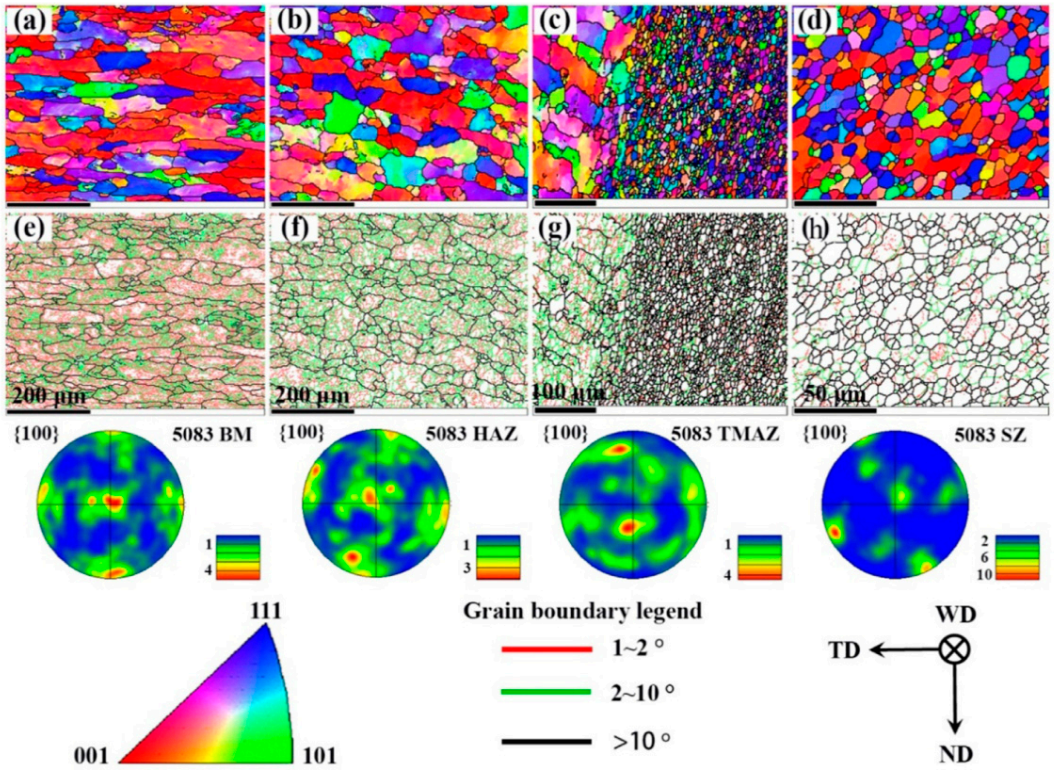

Figure 9. EBSD orientation maps and grain boundaries of the dissimilar AA5083-AA2024 aluminum alloy joint on the AA5083 side: (**a**,**e**) BM, (**b**,**f**) HAZ, (**c**,**g**) TMAZSZ interface and (**d**,**h**) SZ, reproduced from [91], with permission from Elsevier, 2019.

5. Mechanical Properties

5.1. Hardness

The hardness of the FSW joint is related to the joint strength and its deformation behavior, especially in the case of dissimilar material combinations. The hardness distributions of various different Al alloy combinations are shown in Figure 10. The common highly asymmetrical hardness distribution along the cross-section of dissimilar material joints is due to the different microstructural zones (SZ, TMAZ, HAZ) which develop due to the thermo-mechanical history during welding. Since the maximum temperature is reached at the SZ, precipitates or strengthening particles dissolve partially or completely decreasing hardness in SZ. Whereas the lowest hardness values are found in the HAZ due to the coarsening of precipitates or over aging. Therefore, the HAZ always remains the most common zone or site where failure occurs during tensile deformation. It is also worth noting that SZ has higher hardness values compared to the BM (which may be of low strength) because of the combined effect of grain refinement and the effect of both of the BMs in the SZ. However, it is not always true due to different initial conditions of heat-treatable alloy combinations. Recently, Niu et al. [13] reported an interesting hardness behavior of joints prior to and following fracture, by quantifying hardening with the ratio of HV_f/HV_w, where HV_f and HV_w are the microhardness

of the fractured and the as-welded joints, respectively. This ratio was over one in the SZ, TMAZ and HAZ, which confirmed the strain hardened behavior of the joints as shown in Figure 11. In summary, hardness distribution in the dissimilar material joints is closely associated with mechanical behavior such as strain hardening and the fracture origin.

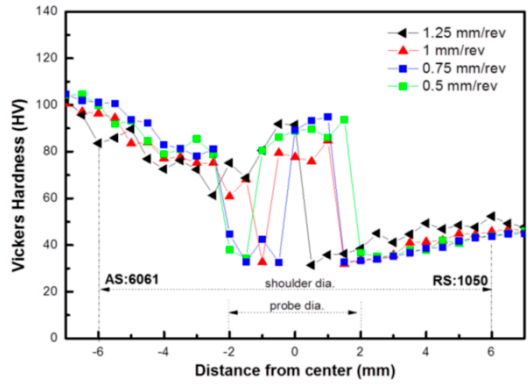

(a) AA6061-AA1050 [42]

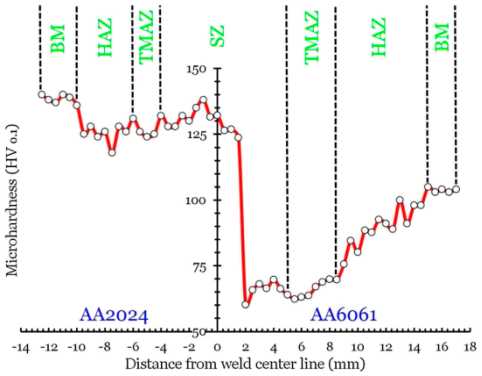

(b) AA2024-AA6061 [22]

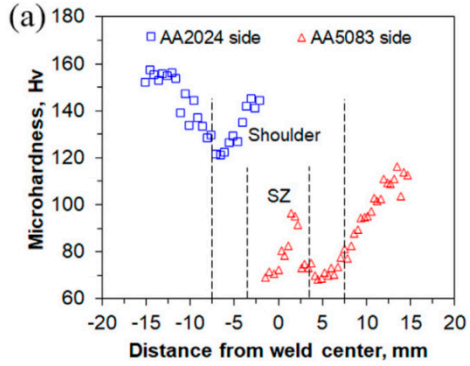

(c) AA2024-AA5083 [91]

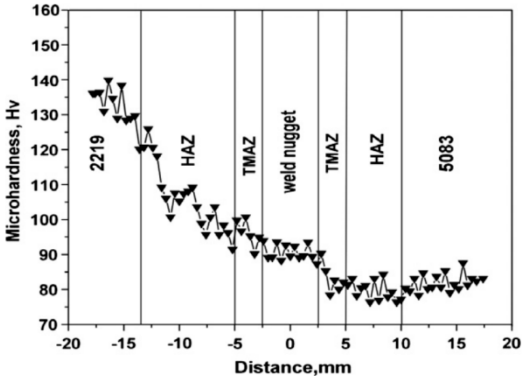

(d) AA2219-AA5083 [60]

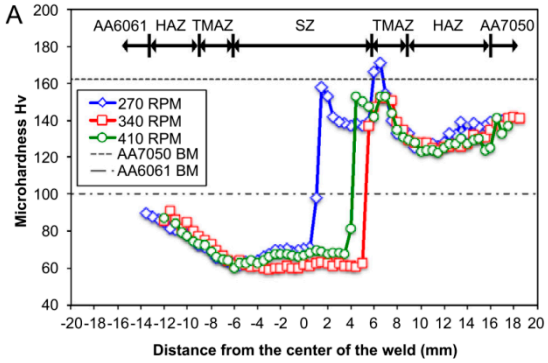

(e) AA6061-AA7075 [46]

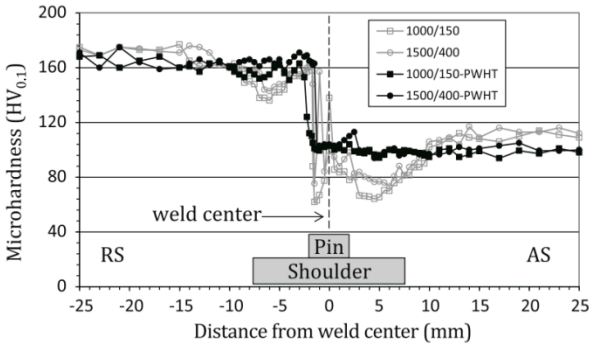

(f) AA6061-AA7075 T6 [51]

Figure 10. Hardness distribution along the cross section of the dissimilar Al combination joints. (**a**) AA6061-AA1050 [42]; with permission from the authors. (**b**) AA2024-AA6061, reproduced from [22], with permission from Elsevier, 2108; (**c**) AA2024-AA5083 reproduced from [91], with permission from Elsevier, 2019; (**d**) AA2219-AA5083 reproduced from [60], with permission from Elsevier, 2012; (**e**) AA6061-AA7075 reproduced from [46], with permission from Elsevier, 2015; (**f**) AA6061-AA7075 T6], reproduced from [51], with permission from Springer, 2014.

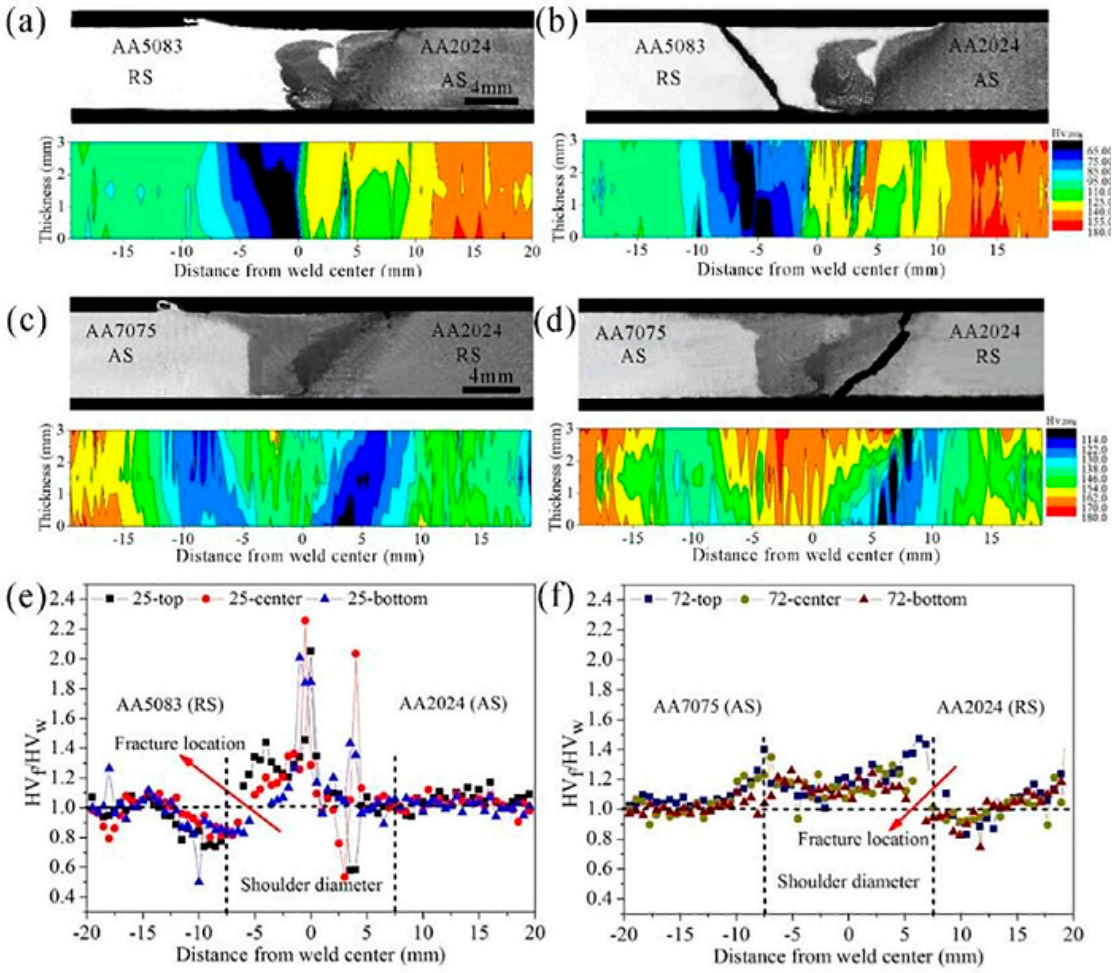

Figure 11. Cross-sectional macrostructures and hardness distributions of the FSWed dissimilar joints: (**a**) 25-joint before fracture, (**b**) 25-joint after fracture, (**c**) 72-joint before fracture, (**d**) 72-joint after fracture; hardening level across the FSWed joints: (**e**) 25-joint and (**f**) 72-joint, reproduced from [13], with permission from Elsevier, 2018. Note: 25-joint means AA2024-AA5083 and 72-joint means AA7075-AA2024 joint.

5.2. Tensile Strength

The number of published papers investigating welding the 5xxx-6xxx series alloys to identify the effect of process parameters (especially the tool rotation speed and welding speed) on the joint strength is shown in detail in Table 1. The joint strength increases with the rotation speed due to the enhanced material mixing effect [18,54,57,62]. The tool rotation speed intensifies plastic deformation and welding speed controls the thermal cycle, residual stresses and rate of production. So, it is essential to select the appropriate combination of these speeds for weld quality or joint strength. Bijanrostami et al. [33] investigated the AA6061-AA7075 joint to identify that maximum joint strength is achieved with a combination of moderate rotation and low welding speed. When high heat input conditions are used (i.e., high rotation and low welding speeds) large grains and lower dislocation densities develop in the SZ. On other side when low heat input condition are selected (i.e., low rotation and high welding speeds) defects are generated. So, grain size strengthening and low dislocation densities are necessary for joint strength. However, the maximum joint strength of an A356-AA6061 joint was achieved with low rotation and welding speed by Ghosh et al. [58,64]. Evidence of fine grain size, fine distribution of Si particles and reduced residual stresses in the SZ were found for low rotation and welding speeds. Together with rotation and welding speeds, the effect of tool geometry like the pin profile or features [14,18,47,48,62], pin shapes [34,57] and shoulder diameter to pin diameter ratio [37,60] on

joint strength have been investigated. The pin profile or feature controls material flow and in effect material mixing at the joint interface, the pin shape affects SZ size as well as material movement and the shoulder to pin diameter ratio controls frictional heat generation between the tool and the BM. The conical threaded pin was identified as the best possible configuration for the AA 6061–AA5086 joint due to the production of a uniformly distributed precipitates and the distinct generation of the onion rings as material was mixed appropriately in the SZ, as reported by Ilangovan et al. [47]. In summary, the tensile strength of the dissimilar FSWed Al joints relies on the microstructure evolution during FSW, which in turn depends on the heat input as governed by the welding parameters (as discussed in Section 4).

6. Summary and Outlook

With regards to the research published and the appropriate future work to be performed in the FSW of dissimilar Al alloy combinations, the following comments can be proposed:

6.1. Al Alloy Combinations

Almost all of the investigations conducted concerned BM in the as-rolled condition that is, 2xxx-5xxx, 2xxx-6xxx, 2xxx-7xxx, 5xxx-6xxx, 5xxx-7xxx Al series. It would be interesting to explore dissimilar Al alloy combinations in as-cast conditions and as a combination between as-cast and as-rolled conditions, depending on the application.

6.2. Base Metal Placement

Limited number of papers on the effect of placement is available and still remains inconclusive. Base material placement becomes an issue in the cases where there are significant differences in mechanical properties of the BMs as in the 6xxx-7xxx and the 5xxx-7xxx combinations.

6.3. Tool Offset

There is a very limited number of welding parameters optimization studies to study tool offset. It needs further comprehensive evaluation using microstructure characterization to understand the material flow in the SZ.

6.4. Bobbing Tool and Stationary shoulder Tool

The bobbin tool [92] and the stationary shoulder tool are considered as a strategic variant of FSW, which have distinct benefits over the conventional FSW tool. Stationary shoulder tool offers low heat input during welding and processing [93–95] and would benefit Al alloy dissimilar joints [96].

6.5. Corrosion and Fatigue Behavior

Finally, corrosion and fatigue behavior studies of various combinations of dissimilar Al alloy joints would be beneficial to expand its industrial use.

Author Contributions: Conceptualization, W.L. and V.P.; methodology, V.P. and P.N. resources, W.L.; data curation, G.W. and F.W.; writing—original draft preparation, V.P.; writing—review and editing, V.P. and AV.; supervision, W.L.; project administration, W.L.; funding acquisition, W.L.

Funding: The authors would like to thank for financial support National Natural Science Foundation of China (51574196, U1637601). We would also like to express our gratitude to the Guest Editor, Antonello Astarita (University of Naples Federico II, Italy) for the invitation to contribute this article to METALS.

Conflicts of Interest: The authors declare no conflict of interest.

References

1. Thomas, W.M.; Nicholas, E.D.; Needham, J.C.; Murch, M.G.; Temple-Smith, P.; Dawes, C.J. Friction Stir Butt Welding. International Patent Application No. PCT/GB92/02203; GB Patent Application No. 9125978.8; U.S. Patent Application No. 5,460,317, 6 December 1991.
2. Mishra, R.; Ma, Z.; Mishra, R. Friction stir welding and processing. *Mater. Sci. Eng. R* **2005**, *50*, 1–78. [CrossRef]
3. Ma, Z.Y.; Feng, A.H.; Chen, D.L.; Shen, J. Recent Advances in Friction Stir Welding/Processing of Aluminum Alloys: Microstructural Evolution and Mechanical Properties. *Crit. Rev. Solid State Mater. Sci.* **2017**, *43*, 269–333. [CrossRef]
4. Gibson, B.; Lammlein, D.; Prater, T.; Longhurst, W.; Cox, C.; Ballun, M.; Dharmaraj, K.; Cook, G.; Strauss, A.; Gibson, B. Friction stir welding: Process, automation, and control. *J. Manuf. Processes* **2014**, *16*, 56–73. [CrossRef]
5. Nandan, R.; Debroy, T.; Bhadeshia, H. Recent advances in friction-stir welding—Process, weldment structure and properties. *Prog. Mater Sci.* **2008**, *53*, 980–1023. [CrossRef]
6. Padhy, G.; Wu, C.; Gao, S. Friction stir based welding and processing technologies - processes, parameters, microstructures and applications: A review. *J. Mater. Sci. Technol.* **2018**, *34*, 1–38. [CrossRef]
7. Shah, P.H.; Badheka, V.J. Friction stir welding of aluminium alloys: An overview of experimental findings—Process, variables, development and applications. *Proc. Inst. Mech. Eng. Part L: J. Mater. Des. Applic.* **2017**, *6*, 1464420716689588. [CrossRef]
8. Wahid, M.A.; Khan, Z.A.; Siddiquee, A.N. Review on underwater friction stir welding: A variant of friction stir welding with great potential of improving joint properties. *Trans. Nonferrous Met. Soc. China* **2018**, *28*, 193–219. [CrossRef]
9. Scherillo, F.; Curioni, M.; Aprea, P.; Impero, F.; Squillace, A.; Zhou, X. Study of the Linear Friction Welding Process of Dissimilar Ti-6Al-4V–Stainless Steel Joints AU - Astarita, Antonello. *Materials and Manufacturing Processes* **2016**, *31*, 2115–2122. [CrossRef]
10. Sepe, R.; Armentani, E.; di Lascio, P.; Citarella, R. Crack Growth Behavior of Welded Stiffened Panel. *Procedia Engineering* **2015**, *109*, 473–483. [CrossRef]
11. Astarita, A.; Prisco, U.; Squillace, A.; Villano, P.; Scherillo, F.; Coticelli, F. Theoretical analysis of a friction stir welded panel in comparison with the baseline version. *Weld. Cutt.* **2016**, *15*, 238–240.
12. Magalhães, V.M.; Leitão, C.; Rodrigues, D.M. Friction stir welding industrialisation and research status. *Sci. Technol. Weld. Joining* **2017**, *23*, 400–409. [CrossRef]
13. Niu, P.; Li, W.; Chen, D. Strain hardening behavior and mechanisms of friction stir welded dissimilar joints of aluminum alloys. *Mater. Lett.* **2018**, *231*, 68–71. [CrossRef]
14. Hasan, M.M.; Ishak, M.; Rejab, M.R.M. Effect of pin tool flute radius on the material flow and tensile properties of dissimilar friction stir welded aluminum alloys. *Int. J. Adv. Manuf. Technol.* **2018**, *98*, 2747–2758. [CrossRef]
15. Ge, Z.; Gao, S.; Ji, S.; Yan, D. Effect of pin length and welding speed on lap joint quality of friction stir welded dissimilar aluminum alloys. *Int. J. Adv. Manuf. Technol.* **2018**, *98*, 1461–1469. [CrossRef]
16. Kalemba-Rec, I.; Kopyściański, M.; Miara, D.; Krasnowski, K. Effect of process parameters on mechanical properties of friction stir welded dissimilar 7075-T651 and 5083-H111 aluminum alloys. *Int. J. Adv. Manuf. Technol.* **2018**, *97*, 2767–2779. [CrossRef]
17. Safarbali, B.; Shamanian, M.; Eslami, A. Effect of post-weld heat treatment on joint properties of dissimilar friction stir welded 2024-T4 and 7075-T6 aluminum alloys. *Trans. Nonferrous Met. Soc. China* **2018**, *28*, 1287–1297. [CrossRef]
18. Palanivel, R.; Laubscher, R.; Vigneshwaran, S.; Dinaharan, I. Prediction and optimization of the mechanical properties of dissimilar friction stir welding of aluminum alloys using design of experiments. *Proc. Inst. Mech. Eng. Part B: J. Eng. Manuf.* **2016**, *232*, 1384–1394. [CrossRef]
19. Hamilton, C.; Dymek, S.; Kopyściański, M.; Węglowska, A.; Pietras, A. Numerically Based Phase Transformation Maps for Dissimilar Aluminum Alloys Joined by Friction Stir-Welding. *Metals* **2018**, *8*, 324. [CrossRef]

20. Gupta, S.K.; Pandey, K.; Kumar, R. Multi-objective optimization of friction stir welding process parameters for joining of dissimilar AA5083/AA6063 aluminum alloys using hybrid approach. *Proc. Inst. Mech. Eng.* **2016**, *232*, 343–353. [CrossRef]
21. Huang, B.W.; Qin, Q.D.; Zhang, D.H.; Wu, Y.J.; Su, X.D. Microstructure and Mechanical Properties of Dissimilar Joints of Al-Mg2Si and 5052 Aluminum Alloy by Friction Stir Welding. *J. Mater. Eng. Perform.* **2018**, *27*, 1898–1907. [CrossRef]
22. Moradi, M.M.; Aval, H.J.; Jamaati, R.; Amirkhanlou, S.; Ji, S. Microstructure and texture evolution of friction stir welded dissimilar aluminum alloys: AA2024 and AA6061. *J. Manuf. Processes* **2018**, *32*, 1–10. [CrossRef]
23. Prasanth, R.S.S.; Raj, K.H. Determination of Optimal Process Parameters of Friction Stir Welding to Join Dissimilar Aluminum Alloys Using Artificial Bee Colony Algorithm. *Trans. Indian Inst. Met.* **2017**, *71*, 453–462. [CrossRef]
24. Azeez, S.; Akinlabi, E. Effect of processing parameters on microhardness and microstructure of a double-sided dissimilar friction stir welded aa6082-t6 and aa7075-t6 aluminum alloy. *Mater. Today: Proc.* **2018**, *5*, 18315–18324. [CrossRef]
25. Azeez, S.; Akinlabi, E.; Kailas, S.; Brandi, S. Microstructural properties of a dissimilar friction stir welded thick aluminum aa6082-t6 and aa7075-t6 alloy. *Mater. Today: Proc.* **2018**, *5*, 18297–18306. [CrossRef]
26. Peng, G.; Ma, Y.; Hu, J.; Jiang, W.; Huan, Y.; Chen, Z.; Zhang, T. Nanoindentation Hardness Distribution and Strain Field and Fracture Evolution in Dissimilar Friction Stir-Welded AA 6061-AA 5A06 Aluminum Alloy Joints. *Adv. Mater. Sci. Eng.* **2018**, *2018*, 1–11. [CrossRef]
27. Das, U.; Toppo, V. Effect of Tool Rotational Speed on Temperature and Impact Strength of Friction Stir Welded Joint of Two Dissimilar Aluminum Alloys. *Mater. Today: Proc.* **2018**, *5*, 6170–6175. [CrossRef]
28. Sarsılmaz, F. Relationship between micro-structure and mechanical properties of dissimilar aluminum alloy plates by friction stir welding. *J. Therm. Sci.* **2018**, *22*, 55–66. [CrossRef]
29. No, K.; Yoo, J.-T.; Yoon, J.-H.; Lee, H.-S. Effect of Process Parameters on Friction Stir Welds on AA2219-AA2195 Dissimilar Aluminum Alloys. *Korean J. Mater. Res.* **2017**, *27*, 331–338. [CrossRef]
30. Hamilton, C.; Dymek, S.; Dryzek, E.; Kopyściański, M.; Pietras, A.; Węglowska, A.; Wróbel, M. Application of positron lifetime annihilation spectroscopy for characterization of friction stir welded dissimilar aluminum alloys. *Mater. Charact.* **2017**, *132*, 431–436. [CrossRef]
31. Kopyściański, M.; Dymek, S.; Hamilton, C.; Weglowska, A.; Pietras, A.; Szczepanek, M.; Wojnarowska, M. Microstructure of Friction Stir Welded Dissimilar Wrought 2017A and Cast AlSi9Mg Aluminum Alloys. *Acta Phys. Pol. A* **2017**, *131*, 1390–1394. [CrossRef]
32. Ghaffarpour, M.; Kazemi, M.; Sefat, M.J.M.; Aziz, A.; Dehghani, K. Evaluation of dissimilar joints properties of 5083-H12 and 6061-T6 aluminum alloys produced by tungsten inert gas and friction stir welding. *Proc. Inst. Mech. Eng.* **2015**, *231*, 297–308. [CrossRef]
33. Bijanrostami, K.; Barenji, R.V.; Hashemipour, M. Effect of Traverse and Rotational Speeds on the Tensile Behavior of the Underwater Dissimilar Friction Stir Welded Aluminum Alloys. *J. Mater. Eng. Perform.* **2017**, *26*, 909–920. [CrossRef]
34. Kasman, S.; Kahraman, F.; Emiralioğlu, A. A Case Study for the Welding of Dissimilar EN AW 6082 and EN AW 5083 Aluminum Alloys by Friction Stir Welding. *Metals* **2016**, *7*, 6. [CrossRef]
35. Palanivel, R.; Laubscher, R.F.; Dinaharan, I.; Murugan, N. Developing a Friction-Stir Welding Window for Joining the Dissimilar Aluminum Alloys AA6351 and AA5083. *Mater. Technol.* **2017**, *51*, 5–9. [CrossRef]
36. Doley, J.K.; Kore, S.D. A Study on Friction Stir Welding of Dissimilar Thin Sheets of Aluminum Alloys AA 5052–AA 6061. *J. Manuf. Sci. Eng.* **2016**, *138*, 114502. [CrossRef]
37. Saravanan, V.; Rajakumar, S.; Banerjee, N.; Amuthakkannan, R. Effect of shoulder diameter to pin diameter ratio on microstructure and mechanical properties of dissimilar friction stir welded AA2024-T6 and AA7075-T6 aluminum alloy joints. *Int. J. Adv. Manuf. Technol.* **2016**, *87*, 3637–3645. [CrossRef]
38. Yan, Z.; Liu, X.; Fang, H. Effect of Sheet Configuration on Microstructure and Mechanical Behaviors of Dissimilar Al–Mg–Si/Al–Zn–Mg Aluminum Alloys Friction Stir Welding Joints. *J. Mater. Sci. Technol.* **2016**, *32*, 1378–1385. [CrossRef]
39. Yan, Z.-J.; Liu, X.-S.; Fang, H.-Y. Fatigue Behavior of Dissimilar Al–Mg–Si/Al–Zn–Mg Aluminum Alloys Friction Stir Welding Joints. *Acta Metall. Sinica* **2016**, *29*, 1161–1168. [CrossRef]
40. Hamilton, C.; Kopyściański, M.; Węglowska, A.; Dymek, S.; Pietras, A. A Numerical Simulation for Dissimilar Aluminum Alloys Joined by Friction Stir Welding. *Metall. Mater. Trans. A* **2016**, *47*, 4519–4529. [CrossRef]

41. Zapata, J.; Toro, M.; López, D. Residual stresses in friction stir dissimilar welding of aluminum alloys. *J. Mater. Process. Technol.* **2016**, *229*, 121–127. [CrossRef]
42. Sun, Y.; Tsuji, N.; Fujii, H. Microstructure and Mechanical Properties of Dissimilar Friction Stir Welding between Ultrafine Grained 1050 and 6061-T6 Aluminum Alloys. *Metals* **2016**, *6*, 249. [CrossRef]
43. Texier, D.; Zedan, Y.; Amoros, T.; Feulvarch, E.; Stinville, J.; Bocher, P. Near-surface mechanical heterogeneities in a dissimilar aluminum alloys friction stir welded joint. *Mater. Des.* **2016**, *108*, 217–229. [CrossRef]
44. Rodriguez, R.; Jordon, J.; Allison, P.; Rushing, T.; Garcia, L. Low-cycle fatigue of dissimilar friction stir welded aluminum alloys. *Mater. Sci. Eng. A* **2016**, *654*, 236–248. [CrossRef]
45. Yoon, T.-J.; Yun, J.-G.; Kang, C.-Y. Formation mechanism of typical onion ring structures and void defects in friction stir lap welded dissimilar aluminum alloys. *Mater. Des.* **2016**, *90*, 568–578. [CrossRef]
46. Rodriguez, R.; Jordon, J.; Allison, P.; Rushing, T.; Garcia, L. Microstructure and mechanical properties of dissimilar friction stir welding of 6061-to-7050 aluminum alloys. *Mater. Des.* **2015**, *83*, 60–65. [CrossRef]
47. Ilangovan, M.; Boopathy, S.R.; Balasubramanian, V. Effect of tool pin profile on microstructure and tensile properties of friction stir welded dissimilar AA 6061–AA 5086 aluminium alloy joints. *Defence Technol.* **2015**, *11*, 174–184. [CrossRef]
48. Reza-E-Rabby, M.; Tang, W.; Reynolds, A.P. Effect of tool pin features on process response variables during friction stir welding of dissimilar aluminum alloys. *Sci. Technol. Weld. Joining* **2015**, *20*, 425–432. [CrossRef]
49. Donatus, U.; Thompson, G.E.; Zhou, X. Anodizing Behavior of Friction Stir Welded Dissimilar Aluminum Alloys. *J. Electrochem. Soc.* **2015**, *162*, C657–C665. [CrossRef]
50. Karam, A.; Mahmoud, T.S.; Zakaria, H.M.; Khalifa, T.A. Friction Stir Welding of Dissimilar A319 and A413 Cast Aluminum Alloys. *Arab J. Sci. Eng.* **2014**, *39*, 6363–6373. [CrossRef]
51. Ipekoğlu, G.; Çam, G. Effects of Initial Temper Condition and Postweld Heat Treatment on the Properties of Dissimilar Friction-Stir-Welded Joints between AA7075 and AA6061 Aluminum Alloys. *Metall. Mater. Trans. A* **2014**, *45*, 3074–3087. [CrossRef]
52. Cole, E.G.; Fehrenbacher, A.; Duffie, N.A.; Zinn, M.R.; Pfefferkorn, F.E.; Ferrier, N.J. Weld temperature effects during friction stir welding of dissimilar aluminum alloys 6061-t6 and 7075-t6. *Int. J. Adv. Manuf. Technol.* **2013**, *71*, 643–652. [CrossRef]
53. Song, Y.; Yang, X.; Cui, L.; Hou, X.; Shen, Z.; Xu, Y. Defect features and mechanical properties of friction stir lap welded dissimilar AA2024–AA7075 aluminum alloy sheets. *Mater. Des.* **2014**, *55*, 9–18. [CrossRef]
54. Jannet, S.; Mathews, P.K. Effect of Welding Parameters on Mechanical and Microstructural Properties of Dissimilar Aluminum Alloy Joints Produced by Friction Stir Welding. *Appl. Mech. Mater.* **2014**, *592*, 250–254. [CrossRef]
55. Palanivel, R.; Mathews, P.K.; Dinaharan, I.; Murugan, N. Mechanical and metallurgical properties of dissimilar friction stir welded AA5083-H111 and AA6351-T6 aluminum alloys. *Trans. Nonferrous Met. Soc. China* **2014**, *24*, 58–65. [CrossRef]
56. Jonckheere, C.; De Meester, B.; Denquin, A.; Simar, A. Torque, temperature and hardening precipitation evolution in dissimilar friction stir welds between 6061-T6 and 2014-T6 aluminum alloys. *J. Mater. Process. Technol.* **2013**, *213*, 826–837. [CrossRef]
57. Palanivel, R.; Mathews, P.K.; Murugan, N. Optimization of process parameters to maximize ultimate tensile strength of friction stir welded dissimilar aluminum alloys using response surface methodology. *J. Cent. South Univ.* **2013**, *20*, 2929–2938. [CrossRef]
58. Ghosh, M.; Husain, M.M.; Kumar, K.; Kailas, S.V. Friction Stir-Welded Dissimilar Aluminum Alloys: Microstructure, Mechanical Properties, and Physical State. *J. Mater. Eng. Perform.* **2013**, *22*, 3890–3901. [CrossRef]
59. Velotti, C.; Squillace, A.; Villano, M.G.; Prisco, U.; Montuori, M.; Giorleo, G.; Astarita, A.; Ciliberto, S.; Giuliani, M.; Bellucci, F. On the critical technological issues of friction stir welding lap joints of dissimilar aluminum alloys. *Surf. Interface Anal.* **2013**, *45*, 1643–1648. [CrossRef]
60. Koilraj, M.; Sundareswaran, V.; Vijayan, S.; Rao, S.K. Friction stir welding of dissimilar aluminum alloys AA2219 to AA5083 – Optimization of process parameters using Taguchi technique. *Mater. Des.* **2012**, *42*, 1–7. [CrossRef]
61. Dinaharan, I.; Kalaiselvan, K.; Vijay, S.; Raja, P.; J, V.S. Effect of material location and tool rotational speed on microstructure and tensile strength of dissimilar friction stir welded aluminum alloys. *Arch. Civ. Mech. Eng.* **2012**, *12*, 446–454. [CrossRef]

62. Palanivel, R.; Mathews, P.K.; Murugan, N.; Dinaharan, I. Effect of tool rotational speed and pin profile on microstructure and tensile strength of dissimilar friction stir welded AA5083-H111 and AA6351-T6 aluminum alloys. *Mater. Des.* **2012**, *40*, 7–16. [CrossRef]
63. Song, S.-W.; Lee, S.-H.; Kim, B.-C.; Yoon, T.-J.; Kim, N.-K.; Kim, I.-B.; Kang, C.-Y. Liquation Cracking of Dissimilar Aluminum Alloys during Friction Stir Welding. *Mater. Trans.* **2011**, *52*, 254–257. [CrossRef]
64. Ghosh, M.; Kumar, K.; Kailas, S.; Ray, A. Optimization of friction stir welding parameters for dissimilar aluminum alloys. *Mater. Des.* **2010**, *31*, 3033–3037. [CrossRef]
65. Kim, N.-K.; Kim, B.-C.; An, Y.-G.; Jung, B.-H.; Song, S.-W.; Kang, C.-Y. The effect of material arrangement on mechanical properties in Friction Stir Welded dissimilar A5052/A5J32 aluminum alloys. *Met. Mater. Int.* **2009**, *15*, 671–675. [CrossRef]
66. Prime, M.; Gnaupel-Herold, T.; Baumann, J.; Lederich, R.; Bowden, D.; Sebring, R. Residual stress measurements in a thick, dissimilar aluminum alloy friction stir weld. *Acta Mater.* **2006**, *54*, 4013–4021. [CrossRef]
67. Miles, M.P.; Nelson, T.W.; Melton, D.W. Formability of friction-stir-welded dissimilar-aluminum-alloy sheets. *Metall. Mater. Trans. A* **2005**, *36*, 3335–3342. [CrossRef]
68. Ouyang, J.H.; Kovacevic, R. Material flow and microstructure in the friction stir butt welds of the same and dissimilar aluminum alloys. *J. Mater. Eng. Perform.* **2002**, *11*, 51–63. [CrossRef]
69. Barbini, A.; Carstensen, J.; Dos Santos, J. Influence of Alloys Position, Rolling and Welding Directions on Properties of AA2024/AA7050 Dissimilar Butt Weld Obtained by Friction Stir Welding. *Metals* **2018**, *8*, 202. [CrossRef]
70. Cavaliere, P.; De Santis, A.; Panella, F.; Squillace, A. Effect of welding parameters on mechanical and microstructural properties of dissimilar AA6082-AA2024 joints produced by friction stir welding. *Mater. Des.* **2009**, *30*, 609–616. [CrossRef]
71. Niu, P.; Li, W.; Li, N.; Xu, Y.; Chen, D. Exfoliation corrosion of friction stir welded dissimilar 2024-to-7075 aluminum alloys. *Mater. Charact.* **2019**, *147*, 93–100. [CrossRef]
72. Rajesh, S.; Badheka, V.J. Process parameters/material location affecting hooking in friction stir lap welding: Dissimilar aluminum alloys. *Mater. Manuf. Process.* **2017**, *33*, 323–332. [CrossRef]
73. Rajesh, S.; Badheka, V.J. Effect of friction stir lap weld and post weld heat treatment on corrosion behavior of dissimilar aluminum alloys. *Proc. Inst. Mech. Eng.* **2017**, *426*. [CrossRef]
74. Rajesh, S.; Badheka, V. Influence of Heat Input/Multiple Passes and Post Weld Heat Treatment on Strength/Electrochemical Characteristics of Friction Stir Weld Joint. *Mater. Manuf. Process.* **2017**, *33*, 156–164. [CrossRef]
75. Mastanaiah, P.; Sharma, A.; Reddy, G.M. Dissimilar Friction Stir Welds in AA2219-AA5083 Aluminium Alloys: Effect of Process Parameters on Material Inter-Mixing, Defect Formation, and Mechanical Properties. *Trans. Indian Inst. Met.* **2015**, *69*, 1397–1415. [CrossRef]
76. Kasman, Ş.; Yenier, Z. Analyzing dissimilar friction stir welding of AA5754/AA7075. *Int. J. Adv. Manuf. Technol.* **2013**, *70*, 145–156. [CrossRef]
77. Forcellese, A.; Simoncini, M.; Casalino, G. Influence of Process Parameters on the Vertical Forces Generated during Friction Stir Welding of AA6082-T6 and on the Mechanical Properties of the Joints. *Metals* **2017**, *7*, 350. [CrossRef]
78. Saeidi, M.; Manafi, B.; Givi, M.B.; Faraji, G. Mathematical modeling and optimization of friction stir welding process parameters in AA5083 and AA7075 aluminum alloy joints. *Proc. Inst. Mech. Eng. Part B: J. Eng. Manuf.* **2015**, *230*, 1284–1294. [CrossRef]
79. Zhu, Z.; Zhang, H.; Yu, T.; Wu, Z.; Wang, M.; Zhang, X. A Finite Element Model to Simulate Defect Formation during Friction Stir Welding. *Metals* **2017**, *7*, 256. [CrossRef]
80. Godhani, P.S.; Patel, V.V.; Vora, J.J.; Chaudhary, N.D.; Banka, R. Effect of Friction Stir Welding of Aluminum Alloys AA6061/AA7075: Temperature Measurement, Microstructure, and Mechanical Properties. In *Innovations in Infrastructure*; Springer: Singapore, Singapore, 2019; pp. 591–598.
81. Zhou, Y.; Chen, S.; Wang, J.; Wang, P.; Xia, J. Influences of Pin Shape on a High Rotation Speed Friction Stir Welding Joint of a 6061-T6 Aluminum Alloy Sheet. *Metals* **2018**, *8*, 987. [CrossRef]
82. Goel, P.; Siddiquee, A.; Khan, N.; Hussain, M.; Khan, Z.; Abidi, M.; Al-Ahmari, A. Investigation on the Effect of Tool Pin Profiles on Mechanical and Microstructural Properties of Friction Stir Butt and Scarf Welded Aluminium Alloy 6063. *Metals* **2018**, *8*, 74. [CrossRef]

83. Patel, V.V.; Badheka, V.; Kumar, A. Friction Stir Processing as a Novel Technique to Achieve Superplasticity in Aluminum Alloys: Process Variables, Variants, and Applications. *Metallogr. Microstruct. Anal.* **2016**, *5*, 278–293. [CrossRef]
84. Patel, V.V.; Badheka, V.; Kumar, A. Effect of polygonal pin profiles on friction stir processed superplasticity of AA7075 alloy. *J. Mater. Process. Technol.* **2017**, *240*, 68–76. [CrossRef]
85. Patel, V.V.; Badheka, V.J.; Kumar, A. Influence of Pin Profile on the Tool Plunge Stage in Friction Stir Processing of Al–Zn–Mg–Cu Alloy. *Trans. Indian Inst. Met.* **2016**, *70*, 1151–1158. [CrossRef]
86. Patel, V.V.; Li, W.Y.; Vairis, A.; Badheka, V.J. Recent Development in Friction Stir Processing as a Solid-State Grain Refinement Technique: Microstructural Evolution and Property Enhancement. *Crit. Rev. Solid State Mater. Sci.* **2019**, accepted. [CrossRef]
87. Dialami, N.; Cervera, M.; Chiumenti, M. Numerical Modelling of Microstructure Evolution in Friction Stir Welding (FSW). *Metals* **2018**, *8*, 183. [CrossRef]
88. Nakamura, T.; Obikawa, T.; Nishizaki, I.; Enomoto, M.; Fang, Z. Friction Stir Welding of Non-Heat-Treatable High-Strength Alloy 5083-O. *Metals* **2018**, *8*, 208. [CrossRef]
89. Aziz, S.A.; Zolkarnain, L.; Rahim, M.A.Z.B.A.; Fadaeifard, F.; Matori, K.A. Effect of the Welding Speed on the Macrostructure, Microstructure and Mechanical Properties of AA6061-T6 Friction Stir Butt Welds. *Metals* **2017**, *7*, 48.
90. Patel, V.V.; Badheka, V.; Kumar, A. Influence of Friction Stir Processed Parameters on Superplasticity of Al-Zn-Mg-Cu Alloy. *Mater. Manuf. Process.* **2015**, *31*, 1–10. [CrossRef]
91. Niu, P.; Li, W.; Vairis, A.; Chen, D. Cyclic deformation behavior of friction-stir-welded dissimilar AA5083-to-AA2024 joints: Effect of microstructure and loading history. *Mater. Sci. Eng. A* **2019**, *744*, 145–153. [CrossRef]
92. Tamadon, A.; Pons, D.J.; Sued, K.; Clucas, D. Thermomechanical Grain Refinement in AA6082-T6 Thin Plates under Bobbin Friction Stir Welding. *Metals* **2018**, *8*, 375. [CrossRef]
93. Wen, Q.; Li, W.; Wang, W.; Wang, F.; Gao, Y.; Patel, V. Experimental and numerical investigations of bonding interface behavior in stationary shoulder friction stir lap welding. *J. Mater. Sci. Technol.* **2019**, *35*, 192–200. [CrossRef]
94. Patel, V.; Li, W.; Xu, Y. Stationary shoulder tool in friction stir processing: a novel low heat input tooling system for magnesium alloy. *Mater. Manuf. Process.* **2018**, *34*, 177–182. [CrossRef]
95. Li, W.; Niu, P.; Yan, S.; Patel, V.; Wen, Q. Improving microstructural and tensile properties of AZ31B magnesium alloy joints by stationary shoulder friction stir welding. *J. Manuf. Process.* **2019**, *37*, 159–167. [CrossRef]
96. Barbini, A.; Carstensen, J.; Dos Santos, J.F. Influence of a non-rotating shoulder on heat generation, microstructure and mechanical properties of dissimilar AA2024/AA7050 FSW joints. *J. Mater. Sci. Technol.* **2018**, *34*, 119–127. [CrossRef]